Journal of Magnetic Resonance 252 (2015) 187–198

Contents lists available at ScienceDirect

Journal of Magnetic Resonance

journal homepage: www.elsevier.com/locate/jmr

Perspectives in Magnetic Resonance

Conformational dynamics of nucleic acid molecules studied by PELDOR spectroscopy with rigid spin labels

T.F. Prisner [a,*], A. Marko [a], S.Th. Sigurdsson [b]

[a] Institute of Physical and Theoretical Chemistry and Center of Biomolecular Magnetic Resonance, Goethe University Frankfurt, Germany
[b] Science Institute, University of Iceland, Reykjavik, Iceland

ARTICLE INFO

Article history:
Received 9 September 2014
Revised 16 December 2014
Available online 20 January 2015

ABSTRACT

Nucleic acid molecules can adopt a variety of structures and exhibit a large degree of conformational flexibility to fulfill their various functions in cells. Here we describe the use of Pulsed Electron–Electron Double Resonance (PELDOR or DEER) to investigate nucleic acid molecules where two cytosine analogs have been incorporated as spin probes. Because these new types of spin labels are rigid and incorporated into double stranded DNA and RNA molecules, there is no additional flexibility of the spin label itself present. Therefore the magnetic dipole–dipole interaction between both spin labels encodes for the distance as well as for the mutual orientation between the spin labels. All of this information can be extracted by multi-frequency/multi-field PELDOR experiments, which gives very precise and valuable information about the structure and conformational flexibility of the nucleic acid molecules. We describe in detail our procedure to obtain the conformational ensembles and show the accuracy and limitations with test examples and application to double-stranded DNA.

1. Introduction

RNA and DNA molecules are important for storage, expression and transmission of the genetic information of living organism. Beside their classical role in translation and transcription, many additional active regulatory and catalytic functions have been found for nucleic acid molecules. Many of these depend not only on the tertiary structure of the molecules but also on the conformational flexibility, which plays an important role in the recognition of cellular cofactors. Riboswitches, ribozymes as well as the whole ribosomal machinery undergo dynamical rearrangements to adopt different states that need to be understood in detail to unravel their functional principles. Whereas X-ray crystallography is very successful to elucidate the 3D-structure of such molecules in specific functional states, spectroscopic methods are used to investigate the dynamics of nucleic acids [1]. NMR spectroscopy is a very powerful tool to get detailed structural and dynamic information with atomistic resolution [2–7]. The distance range that can be addressed directly by NMR is restricted to about 2 nm, additionally the overall size of the biomolecule is restricted to about 30 KD. Fluorescence spectroscopy allows investigation of sup-picosecond time scales with single molecule sensitivity. FRET (Förster Resonance Energy Transfer) allows investigation of distances between two attached chromophores up to 10 nm [8,9]. Unfortunately in many cases its accuracy is limited by unknown fit parameters and the size and flexibility of the fluorophores to sub-atomistic resolution only.

PELDOR (Pulsed Electron–Electron Double Resonance) allows the determination of magnetic dipole–dipole interaction between two unpaired electron spins in solids. First introduced to measure intermolecular dipolar interactions on statistically distributed radical samples [10,11] it is nowadays mostly used to measure intra-molecular distances between two spin labels attached to a molecule. This aspect was emphasized and demonstrated on a model compound, where the method was renamed to DEER (Double Electron–Electron Resonance) [12] and extended to the nowadays almost exclusively 4-pulse DEER sequence [13,14]. With the invention of site-specific spin-labeling [15] it soon became obvious that this experiment is a powerful tool for structural investigations in disordered protein samples [16]. Today it is a standard tool for distance determinations on the 1–10 nm length scale in many macromolecular systems, ranging from polymer and surface sciences to structural biology [17–21]. Nitroxide spin labels are most commonly used [22,23], but also natural occurring cofactors [24,25] amino acid radicals [26],[27] [28], metal centers [29,30], iron-sulfur clusters [31,32], or rare earth metal tags [33–35] have been used as paramagnetic centers.

Intrinsic protein bound paramagnetic cofactors are usually rigidly attached. At high magnetic fields the anisotropy of the

* Corresponding author.
E-mail address: prisner@chemie.uni-frankfurt.de (T.F. Prisner).

http://dx.doi.org/10.1016/j.jmr.2014.12.008
1090-7807/

g-tensor can be used with the narrowband microwave excitation pulses to select a subset of molecules at specific orientations with respect to the external magnetic field. In this case, not only the distance between the paramagnetic cofactors, but also their mutual orientation can be extracted from PELDOR experiments. This was first demonstrated for two tyrosine radicals of dimeric ribonucleotide reductase [26,28]. In the case of flexible spin labels, such as the MTSSL spin label attached to cysteines amino acid residues, this orientation information is usually averaged out and the distance distribution function $P(r)$ can be extracted directly from PELDOR time trace by Tikhonov regularization methods [36–38]. The DeerAnalysis and MMM simulation programs developed by Jeschke et al. [39] are excellent tools used by many scientists to quantitatively analyze and interpret such experimental data and to compare the results with predictions based on X-ray structures or models. If more than two spin labels are attached to the macromolecule, the interpretation of the PELDOR time traces become more cumbersome [40,41]. However, valuable information on the number of spin labels, for example the oligomeric state of protein complexes can still be obtained [42,43]. If the spin labels are rigid, meaning that they adapt only one well defined conformation with respect to the biomolecule, additional information about the geometry of the coupled spins and therefore the protein symmetry can be obtained by comparison with simulations [44–47]. In this paper we describe how the incorporation of rigid spin labels into DNA and RNA molecules allow determination of very detailed information on the distance vector ***r*** between both radicals, as well as on their relative orientation, described by a set of Euler angles ***o***. This not only increases the information content of a doubly-labeled nucleic acid molecule by a factor of six but in addition strongly enhances the accuracy of the structural information of the nucleic acid molecule itself as there is no internal degree of freedom associated with the spin label. We describe our approach starting from the synthesis of specific rigid spinlabels, the multi-frequency and multi-field experimental approach and finally the simulation procedure developed to accurately determine all six parameters independently. Some illustrative examples will demonstrate both the accuracy and also some limitations of this approach for rigid and flexible macromolecules with two spin labels attached. Finally we will discuss potential applications and extensions of this method.

2. Synthesis of rigid spin labels for nucleic acids

Before pulsed EPR spectroscopy took center stage, continuous wave (CW) EPR was used to study structures of biomolecules by estimation of relatively short distances (ca. 10–25 Å) through line-shape analysis [48]. In addition, there was evidence that EPR spectroscopy of nitroxides could be used to obtain information about orientations in biopolymers. Specifically, CW-EPR spectroscopy of nitroxides has been used to obtain information about orientations in biopolymers. Hustedt and coworkers used CW-EPR at 9.8, 34, and 94 GHz to evaluate distances and orientations of the monomers in a tetrameric complex of glyceraldehyde-3-phosphate dehydrogenase [49]. This was made possible by the fact that the spin labeled NAD^+ cofactor was immobilized upon binding to the enzyme. The promise of being able to obtain additional structural insights through orientation information called for a general approach to extract orientation information in addition to distance distributions. This required a strategy for incorporating rigid spin labels i.e. that do not move independently of the site of attachment.

Nucleic acids are biopolymers that contain well-defined helical elements which are ideal structural scaffolds for accommodating rigid spin labels. Given the abundance of helical elements both in DNA and in RNA, this would provide a strategy to study three-dimensional structures of nucleic acids. Hopkins and co-workers had previously synthesized the rigid spin label Q for DNA, however the spin label was a *C*-nucleoside that required a lengthy synthesis and base-paired with the non-natural nucleoside 2-aminopurine [50]. Our approach was to use a phenoxazine scaffold, which is an analog of cytidine that forms base-pairs with G. This moiety has already been shown by Matteucci and coworkers to fit well within nucleic acid duplexes [51]. The phenoxazine ring-system was simply extended to include a five-membered nitroxide ring producing the nucleoside **Ç** ("C-spin") (Fig. 1) [52].

The strategy to synthesize **Ç** is shown in Fig. 1B [52]. In short, the oxygen atom in position 4 of acetyl-protected 5-iodouridine **1** was converted into a leaving group and displaced by the isoindoline derivative **3**. After ring closure and deprotection, nucleoside **Ç** was obtained and subsequently protected in the 5-position and phosphitylated to produce phosphoramidite **4**, a building block for chemical synthesis of deoxyoligonucleotides. A similar strategy was used to prepare the phosphoramidite **5** of the ribo-derivative for **Çm** for synthesis of RNA, which contains a methoxy group in the 2′-position of the sugar [53].

Phosphoramidite **4** was used to synthesize several oligonulceotides for characterization of DNAs containing **Ç** [54]. Circular dicroism measurements showed characteristic spectra for B-form DNA. Thermal denaturation experiments showed a similar melting point of duplexes containing either **Ç** or C paired with G, indicating that no structural deformation is caused by the spin label. On the other hand, when **Ç** was paired with either A, C or T, the melting temperature was 10–15 °C lower, showing that **Ç** needed to pair with G to form a stable base pair. EPR spectra of the spin labeled duplexes were also recorded and showed a dramatic increase in the spectral width, compared to the nucleoside or the single strand (Fig. 2A). In fact, the spectral width of a **Ç**-labeled DNA duplex could be modeled using the rotational correlation times expected for a cylinder with the dimensions of a DNA duplex [52,52,55]. The spin label **Çm** was also incorporated into several different RNAs and was similarly found to be a non-perturbing label for RNA [53].

PELDOR was also used to measure a series of distances between pairs of **Ç** labels in DNA (Schiemann, 2009) [56] and pairs of **Çm** in RNA [57], which were in good agreement with modeled distances. However, the ultimate proof of the non-perturbing nature of non-natural nucleosides is a high-resolution structure of a duplex containing the modification. We were able obtain a crystal structure of an A-form DNA containing Ç that diffracted to 1.7 Å. This structure showed that **Ç** does indeed form a non-perturbing base-pair with G with the nitroxide moiety projecting into the major groove without causing any steric clashes (Fig. 2B) [58].

3. The PELDOR method

Several reviews and textbooks exist which describe the method [17] [59] and its applications to macromolecular systems such as proteins [18] and nucleic acids [19,60–62] in detail. Therefore, here we will concentrate only on how to obtain angular information from the method of using rigid spin labels incorporated into nucleic acid molecules. The magnetic dipole–dipole interaction frequency ω_d between the unpaired electron spins of two spin labels attached to the nucleic acid molecule is measured by PELDOR spectroscopy. The dipolar coupling strength ω_d (in frequency units) is determined by the distance r and the orientation θ of the inter-spin vector ***r*** with respect to the external magnetic field B_0 by,

$$\omega_d(r,\theta) = \frac{D}{r^3}(1 - 3\cos^2\theta). \quad (1)$$

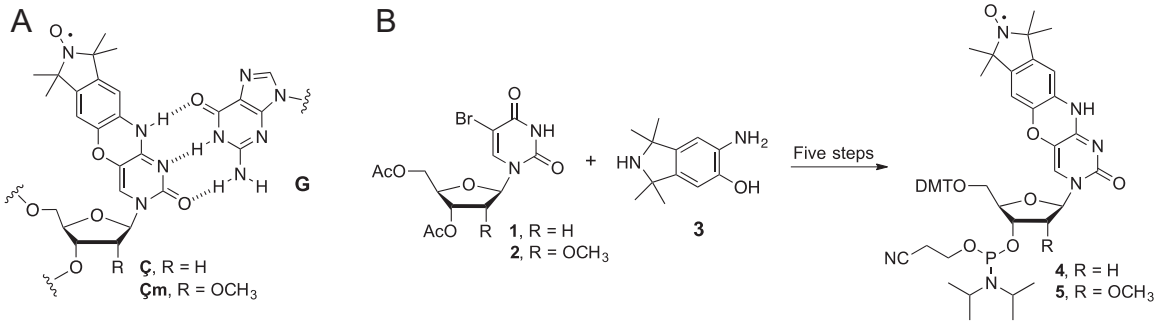

Fig. 1. Rigid spin labels for nucleic acids. (A) Structures of **Ç** and **Çm** and their base-pairing to guanine (**G**). (B) Outline of the syntheses of the phosphoramidites of **Ç** and **Çm**, **4** and **5** respectively.

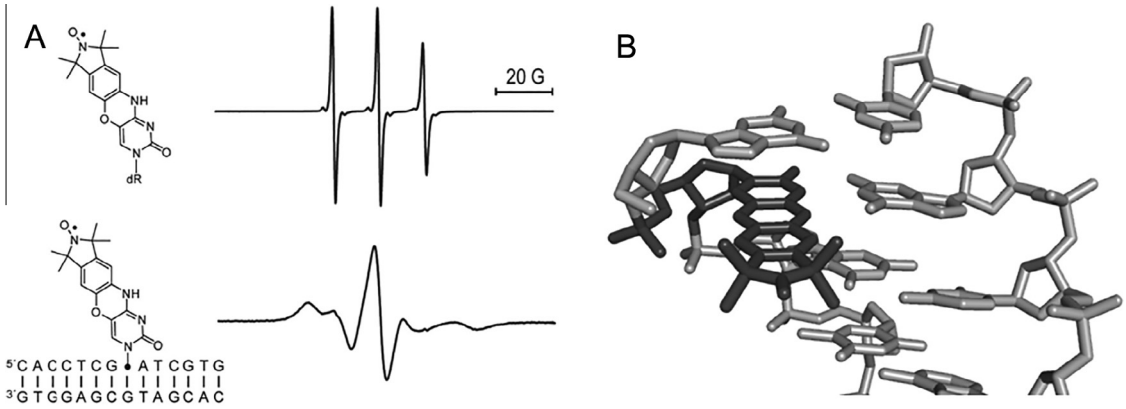

Fig. 2. CW-EPR and X-ray structure of **Ç**. (A) EPR spectrum of **Ç** and a 14-mer duplex DNA containing **Ç**. (B) Crystal structure of **Ç** in duplex DNA.

Here $D = \mu_0\mu_B^2 g_A g_B/(4\pi\hbar)$ is the dipolar interaction constant, wherein μ_0 is the magnetic susceptibility constant of vacuum, μ_B is the Bohr magneton and $\hbar$ is the reduced Planck constant. For nitroxide spin labels, the g-values g_A and g_B correspond to 2.006 resulting in a value of the dipolar constant $D = 2\pi \cdot 52.04$ MHz nm^3. In the original form the PELDOR pulse sequence consist of the three mw-pulses (3-pulse PELDOR) [11], including a Hahn-echo sequence applied at the frequency ν_A and an inversion pulse applied at the frequency ν_B (Fig. 3). Spins resonant with the probe frequency ν_A and pump frequency ν_B are called *A*- and *B*-spins, respectively. The experiments are usually performed using dilute samples (ca. 100 μM concentration of double labeled nucleic acid molecules), so that in a first view single spin pairs consisting of one *A*- and one *B*-spin can be considered and intermolecular interactions can be neglected. Whereas the Hahn-echo sequence refocuses all probe *A*-spin interactions, the inversion pulse applied at pump frequency ν_B, applied a time T after the initial $\pi/2$-pulse, flips the coupled *B*-spin. This changes the Larmor frequency of the *A*-spin by $\pm\omega_d$, depending on the specific spin state of the *B*-spin before the inversion pump pulse [63]. Since the populations of *B*-spins with spin up and down are almost equal in the high temperature limit, the number of *A*-spins which angular frequency accelerated by $+\omega_d$ is equal to the number of *A*-spins whose angular frequency is reduced by $-\omega_d$. Therefore, due to the precession frequency shift caused by the pump pulse one half of the *A*-spins refocus at time 2τ with the phase $+\omega_d T$ whereas the other half refocuses with the phase $-\omega_d T$. The total transversal magnetization of the *A*-spin echo at time 2τ can therefore be represented as the sum of two vectors precessing in opposite directions, with angles depending on the delay T, i.e.

$$M(T) = \frac{1}{2}\left(e^{i\omega_d T} + e^{-i\omega_d T}\right) = \cos(\omega_d T). \quad (2)$$

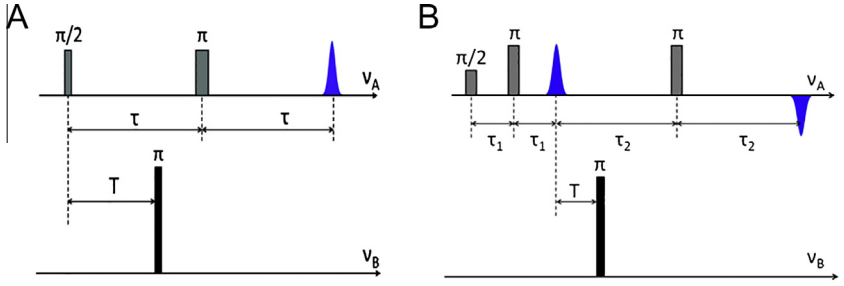

Fig. 3. PELDOR pulse sequences. (A) 3-pulse and (B) 4-pulse PELDOR sequences with probe pulses at frequency ν_A and pump pulse at frequency ν_B. The Hahn-echo at time 2τ (A) and the refocused Hahn-echo at time $2(\tau_1 + \tau_2)$ (B) are modulated by the pump pulse applied at time T.

Therefore the probe spin echo signal is modulated in amplitude by the dipolar interaction frequency as a function of T describing the PELDOR signal time trace recorded in such experiments.

Due to the technical problems in the 3-pulse PELDOR experiment the signal cannot be detected for short times T when the pump pulse is very close to the probe pulse. As this part of the signal is rather important for accurate data analysis and the determination of short distances between the spin labels, the 4-pulse version [13,14], which overcomes this problem, is almost exclusively used nowadays. An additional π-probe pulse is added to refocus the first Hahn echo and the PELDOR time domain signal is recorded as a function of the time T which has its time zero now at the first Hahn echo, where no probe pulses occur. Phase cycling and stepping of the time τ_1 between the first and the second probe pulse are done to suppress hyperfine modulations and experimental ring-time artifacts in the PELDOR time trace.

In reality identical spin labels are used at both labeling positions of the nucleic acid molecule and the differentiation, which spin is A- and which B-spin is specified by the distinct resonance frequencies ν_A and ν_B, which select specific orientation and nuclear spin states of the nitroxide radicals, defined by the anisotropy of the g- and hyperfine A-tensors. This requires that the excitation bandwidth of the microwave pulses applied at frequency ν_A and ν_B are narrower that the frequency difference $\Delta\nu_{AB} = \nu_A - \nu_B$. Therefore, the probability p that a B-spin coupled to a A-spin is flipped by the inversion pulse is smaller than one. The PELDOR time domain signal thus consists of a constant non-modulated part with the amplitude $1-p$ and a part oscillating with the dipolar interaction frequency $p\ cos(\omega_d T)$.

Two situations can be distinguished: in the first case, the spin label attached to the nucleic acid is flexible, thus allowing random mutual orientation between both spin labels. In this case the probability p can easily be calculated from the known excitation profiles of the mw pulses and the g- and A-tensors for nitroxide radicals. Because of the random orientation between both nitroxides, the full dipolar Pake pattern is excited and only the distance information can be extracted from the PELDOR time traces, for example by Tikhonov regularization methods [38,36,37]. In the second case, both spin labels are rigidly incorporated into the nucleic acid molecule. Thus, the distance r as well as the relative orientation between both spin labels contributes to the oscillation frequency in the PELDOR time trace. Additionally, the flip probability of the B-spin coupled to the A spins selected by the probe frequency ν_A in such rigid samples depend on the specific orientation of the dipolar vector $\boldsymbol{r}$ in the external magnetic field, which can be described by a distribution function $\lambda(\theta)$ [12,64,44]. The overall PELDOR signal from a random oriented powder ensemble of rigid nucleic acid molecules with two rigidly attached spin labels can be described by the expression:

$$S(T) = e^{-\gamma T}\left(1 - \int_0^{\pi/2} \lambda(\theta)(\cos(\omega_d(r,\theta)T) - 1)\sin\theta d\theta\right), \tag{3}$$

where the factor $\exp(-\gamma T)$ with $\gamma = 8\pi^2\ p\ c\ D/(9\cdot 3^{1/2})$ describes the intermolecular signal decay by the randomly distributed molecules in the sample, where c is the spin concentration. All other terms have been already defined above.

4. Angular information in PELDOR spectroscopy

To calculate the PELDOR signal for a powder sample with a given fixed orientation between the A- and B-spin, a coordinate system is used with the z-axis parallel to the interspin connecting vector $\boldsymbol{r}$. The direction of the external magnetic field is defined by two polar angles θ and ϕ in this coordinate system and the orientation of each nitroxide by a set of Euler angles $\boldsymbol{o_1}$ and $\boldsymbol{o_2}$ (Fig. 4).

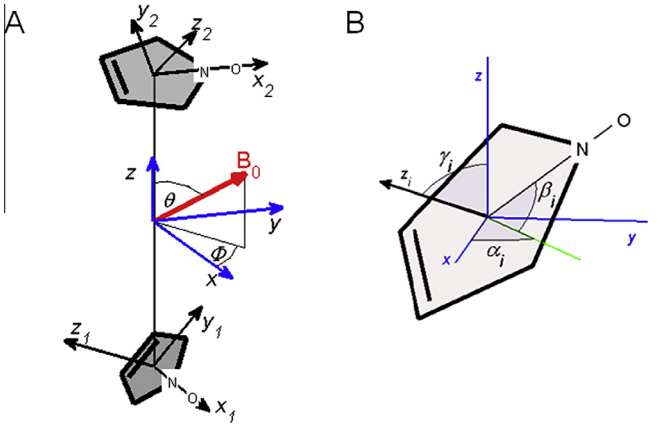

Fig. 4. Coordinate system and angles defining the geometry of two dipolar coupled nitroxide spin labels. (A) Shown is the main axis system (x, y, z, blue) related to the distance vector $\boldsymbol{r}$, the polar angles (θ, ϕ) defining the orientation of the external magnetic field vector $\boldsymbol{B}_0$ (red) and the molecular axis systems of both nitroxides (x_1, y_1, z_1 and x_2, y_2, z_2, in black). (B) The set of Euler angles (α_i, β_i, γ_i) of nitroxide i (i = 1 or 2) defining the orientation of the nitroxide with respect to the main axis system (x, y, z).

In this coordinate system the Larmor frequency of an electron spin is described by the anisotropy of the nitrogen hyperfine tensor $\boldsymbol{A}$ and the $\boldsymbol{g}$-tensor:

$$\omega_r(\theta,\Phi,o,m) = \gamma_e\left(B_0\frac{g_{eff}(\theta,\Phi,o)}{g_e} + mA_{eff}(\theta,\Phi,o) + \delta b\right). \tag{4}$$

The nuclear spin state of the nitrogen atom (^{14}N, I = 1) is described by the quantum number m. The effective g- and hyperfine A-value for the given orientation is denoted by g_{eff} and A_{eff}, respectively. An additional shift of the Larmor frequency, for example due to other nuclear spins, is taken into account by the quantity δb, which gives rise to inhomogeneous line-broadening.

The probability of a B-spin to flip under the effect of the pump pulse is given by [65–67]:

$$p(\omega_r,\nu_B) = \frac{1}{2}\left[\frac{\gamma_e B_{1B}}{\Omega_B(\omega_r)}\right]^2(1-\cos(\Omega_B(\omega_r)t_\pi^B)), \tag{5}$$

where t_π^B is the length of the π-pump pulse and $\Omega_B(\omega_r)$ the Rabi frequency of an electron spin with a Larmor frequency ω_r under the effect of a microwave field B_{1B} with frequency ν_B, defined by:

$$\Omega_B(\omega_r) = \sqrt{\gamma_e^2 B_{1B}^2 + (2\pi\nu_B - \omega_r)^2}. \tag{6}$$

Similarly, the magnitude of the transversal magnetization of the probe A-spins with a Larmor frequency ω_r for a refocused echo pulse sequence with the microwave frequency ν_A is expressed by:

$$m_x(\omega_r,\nu_A) = \frac{1}{4}\left[\frac{\gamma_e B_{1A}}{\Omega_A(\omega_r)}\right]^5 \sin(\Omega_A(\omega_r)t_{\pi/2}^A)(1-\cos(\Omega_A(\omega_r)t_\pi^A))^2. \tag{7}$$

Here $t_{\pi/2}^A$ and t_π^A are the lengths of the $\pi/2$- and π-probe pulses, respectively and $\Omega_A(\omega_r)$ describes the Rabi oscillation frequency as defined above for the B-spins. The formulas for the transversal magnetization m_x and for the spin flip probability p both contain the Larmor resonance frequency ω_r which depend on the magnetic field orientation (described by θ and ϕ) with respect to the nitroxide orientation (given by the Euler angles $\boldsymbol{o_1}$ and $\boldsymbol{o_2}$). Thus both functions $m_x(\omega_r, \nu_A)$ and $p\ (\omega_r, \nu_B)$ depend strongly on orientations. They achieve their maxima for the angles θ, ϕ, $\boldsymbol{o}$ and the nuclear spin quantum number m, that together satisfy the conditions $\omega_r(\theta, \phi, \boldsymbol{o}, m) = 2\pi\nu A$ or $\omega_r(\theta, \phi, \boldsymbol{o}, m) = 2\pi\nu B$. Roughly speaking, nitroxide

molecules which are oriented in such a way that their resonance frequencies differ more than $\gamma_e B_{1A}$ from ν_A and more than $\gamma_e B_{1B}$ from ν_B remain virtually unexcited by the microwave pulses.

For the magnetic field B_0, oriented in the direction θ, ϕ in the biradical frame, the resonance frequencies are calculated from the formulas $\omega_{r1} = \omega_r(\theta, \phi, \boldsymbol{o}_1, m_1)$ and $\omega_{r2} = \omega_r(\theta, \phi, \boldsymbol{o}_2, m_2)$ for the first radical with the nuclear magnetic spin quantum number m_1 and the second radical with the nuclear spin quantum number m_2, respectively. The function λ is an averaged sum of the A-spin echo magnetization, multiplied with the flip probability of the B-spins:

$$\lambda(\theta) = \frac{1}{2V(\nu_A)} \sum_{m_1,m_2} \langle m_x(\omega_{r1}, \nu_A) p(\omega_{r2}, \nu_B) + m_x(\omega_{r2}, \nu_A) p(\omega_{r1}, \nu_B) \rangle_{\phi,\delta b_1,\delta b_2}. \quad (8)$$

$V(\nu_A)$ is the spin echo magnetization in the absence of the pump pulse. Finally the PELDOR signal for a powder sample with random orientation of molecules in the frozen solution is obtained by integration over all θ angles:

$$S(T) = \frac{1}{N} \sum_{i=1}^{N} \left(1 - \int_0^{\pi/2} \lambda_i(\theta) (\cos(\omega_d(r_i, \theta) T) - 1) \sin\theta d\theta \right). \quad (9)$$

The sum allows the molecule to adapt N distinct conformers with specific geometries between the two nitroxide radicals.

5. Procedure to disentangle distance and orientation information

If the structure of the molecule is known, a quantitatively prediction of the expected PELDOR time trace $S(T)$ can easily be obtained, because most of the other parameters in the formula are experimentally well known. Experimental parameters, as for example the excitation profile of the microwave pulse sequences applied at frequency ν_A, have been experimentally obtained with a 1 mm small single crystal of a $(\text{flouranthenyl})_2^+(\text{PF}_6)_{0.5}^-(\text{SbF}_6)_{0.5}^-$ one dimensional organic conductor crystal with a narrow homogeneous linewidth of 3 μT [68]. The signal intensity of this sample was measured for all possible frequency offsets and sample positions inside of the microwave cavity to obtain the experimental excitation profiles. From these profiles empirical Gaussian functions that fit the overall excitation shape of an extended volume sample have been constructed and used for the simulations of PELDOR time traces. Most of the spin parameters for the used nitroxide radicals are also well known. The main g-tensor values as well as the large hyperfine component A_{zz} are known from a high field (6.4 T) EPR spectrum of a powder sample at low temperatures and the isotropic hyperfine coupling constant A_{iso} from room-temperature cw-EPR spectra. Therefore there remains only some freedom in the choice of the inhomogeneous linewidth parameter (δb), modeling the couplings to other nuclear spins, and of the two small hyperfine components A_{xx} and A_{yy}, which do not affect the simulations much if the pulse excitation bandwidths are larger than these parameters.

Structural predictions obtained by other methods, for example molecular dynamic (MD) simulations or NMR, can be directly used to generate simulated PELDOR time traces. These simulated traces can then be quantitatively compared with the experimental PELDOR signals. This is especially true for the rigid spin labels discussed here, because they do not introduce additional degrees of freedom and can easily be modeled into structures obtained from MD or NMR. This is not so easy with flexible spin labels such as MTSSL, which are used for most protein applications since they can adapt different rotameric states introducing additional uncertainties by *per-se* unknown population and distributions of the rotameric states. In such cases the expected absolute accuracy between predicted and measured distances is in the range of 0.3 nm [18,69] as evaluated from known protein structure databanks.

Approaching the problem the other way around, extracting the relative orientation and distance between the two nitroxide spin labels from the PELDOR time traces directly, is not so straight forward. Thus far it has not been possible to derive a closed mathematical relation which would allow a direct determination of the Euler angles $\boldsymbol{o}$ between both spin labels and the distance vector $\boldsymbol{r}$ from the recorded PELDOR time traces. This statement especially holds if more than one conformer of the nucleic acid oligonucleotide coexists. Additional ambiguity is usually introduced by the fact that the two attached spin labels are indistinguishable (both can serve as A- or B-spin).

To obtain unique solutions of all six parameters describing a given geometry, a single PELDOR time trace is usually not sufficient, because it does not obtain enough independent information. Instead several PELDOR experiments performed at different pump/probe frequencies (multi-frequency PELDOR) and at different magnetic field strengths B_0 (multi-field PELDOR) are required to obtain a specific fingerprint for a given structure. Usually we perform multi-frequency/multi-field PELDOR experiments as illustrated in Fig. 5. At low field (0.3 T), where the hyperfine anisotropy dominates the spectral width of about 200 MHz, the probe frequency is changed while the pump frequency stays in the center of the spectrum (to obtain maximum modulation depth). At high magnetic fields (6.4 T) the overall spectral shape with a width of about 600 MHz is fully dominated by the anisotropic g-tensor. In this case the pump and probe frequency are kept at a constant offset (typically 70 MHz) within the bandwidth of the microwave resonator and the magnetic field is systematically changed to obtain resonance conditions at different spectral positions. Using this procedure, different well-known subsets of orientation of the molecules with respect to the external magnetic field are selected, allowing examination of the orientation dependence of the dipolar interaction frequency and modulation depth. From this data the orientation of the interconnecting vector $\boldsymbol{r}$ with respect to the molecular axis systems of the two nitroxide radicals can be deduced. If no angular correlation exist all such recorded PELDOR time traces will exhibit the same oscillation frequencies. On the other hand variations are an inevitable signature that angular correlations exist.

This so called 'orientation selection' has been used in a similar way in hyperfine spectroscopy to correlate anisotropic hyperfine tensors A with the anisotropic g-tensor axis system [70,71]. It allows the selection of different well-ordered, single-crystal like sub-ensembles out of a disordered powder sample and significantly increases the information content of the obtained data.

To tackle the problem of finding the conformations of a molecule directly from such PELDOR time traces, we constructed a multi-frequency/multi-field library of PELDOR signals containing all possible geometries between two nitroxides [72,63,73]. To prepare the PELDOR database, the function $\lambda(\theta)$ was calculated for arbitrary Euler angles $\boldsymbol{o}$ (with 10° steps for all angles). This allows computation of the PELDOR signals for any given biradical with an interspin distance r. Signals for other distances can be obtained simply by rescaling the time axis. Thus, each possible conformation of a molecule is presented in the resulting database by a set of signals, corresponding to the various experimental conditions, e.g. different pump–probe frequency offsets and different magnetic field values. Solutions are found by a simultaneous comparison of all experimental time traces with the database signals. The conformation which has the smallest deviation from the experimental PELDOR time traces is selected as a solution. For a molecule with a single rigid conformation unique solutions can be easily found

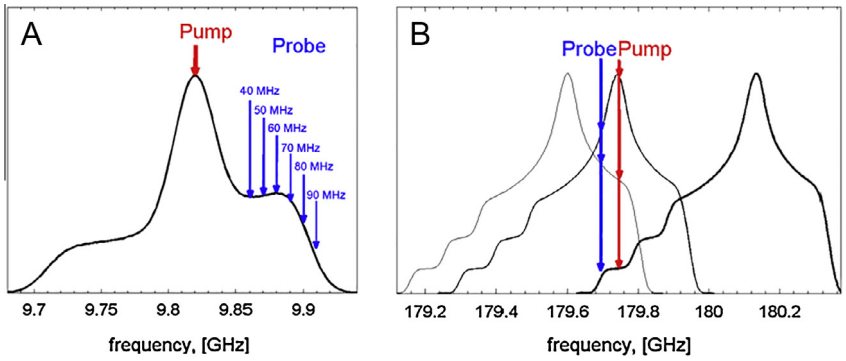

Fig. 5. Selection of pump and probe frequencies for multi-frequency PELDOR. (A) Typical pump and probe positions of the orientation selective X-band PELDOR experiment and (B) field sweep method used for orientation selective G-band PELDOR experiments with a fixed pump–probe frequency offset of 70 MHz.

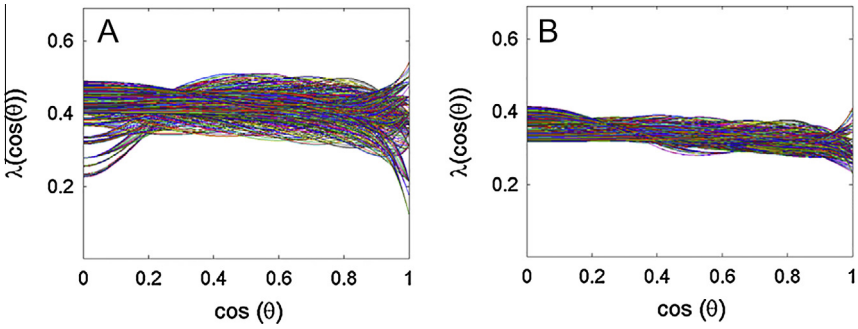

Fig. 6. Angular dependence of the pump efficiency. The pump efficiency functions $\langle\lambda_i\rangle_v$ as a function of the dipolar angle θ shown for all possible relative orientations between two nitroxides. (A) Averaged values over probe–pump frequency offsets ranging from 40 to 90 MHz. (B) Averaged values over probe–pump frequency offsets ranging from 30 to 90 MHz. For more details see explanation in the text.

with this procedure [72,63]. For more flexible molecules which can adopt several conformers the fit program selects iteratively an ensemble of conformers to fit the experimental time traces. Ensembles which satisfactorily fit the experimental data sets are always found but it is not trivial to prove the uniqueness of the solution, as will be shown exemplarily below.

The presence of orientation information in PELDOR signals provides valuable additional structural restraints. However, as Eq. (3) shows, an unknown non-constant value of $\lambda(\theta)$ complicates the determination of the distance distribution function. In order to avoid orientation selection artifacts in the distance distribution it was suggested to average the time traces obtained under varied pump or probe frequency offsets and to take this averaged time domain signal as input for the computation of the distance distribution function [38]. The quality and reliability of such a procedure can be easily evaluated using all the synthesized time traces of our PELDOR database. For this we calculated $\langle\lambda_i\rangle_v$, which is the orientation intensity function averaged over all different pump–probe offsets for all 1045 different conformers (i) of our database (Fig. 6).

On the left (A) six time traces with equally spaced frequency offsets ranging from 40 to 90 MHz have been averaged. The pump pulse with a length of 12 ns was set to the center of the nitroxide spectrum. In the second simulation on the right side (B) seven different frequency offsets have been averaged, ranging from 30 to 90 MHz. In comparison to the first simulation, the length of the pump pulse has been extended to 20 ns to avoid too severe spectral overlap of the pump and probe pulse for the small offset of 30 MHz. In the ideal case of complete averaging of orientation selection effects the functions $\langle\lambda_i\rangle_v$ has to be constant with respect to θ for all conformers i. Fig. 6 shows that indeed the averaged values $\langle\lambda_i\rangle_v$ show considerably less amplitude changes as a function of θ compared to the non-averaged λ functions (see Fig. 7 for comparison). The simulations show that averaging of seven time traces with the shortest offset set to 30 MHz will reduce the deviations of the $\langle\lambda_i\rangle_v$ functions from an average value even more. This can be explained by the more homogeneous excitation of probe spin orientations by extension of the probe spin frequency ν_A to the center of the nitroxide spectrum. In any case, the deviations of the functions $\langle\lambda_i\rangle_v$ from an average value are small enough to be neglected in practical applications.

Because these offset-averaged intensity functions $\langle\lambda_i\rangle_v$ are all equal and independent of θ we are now able to obtain the classical equation for such offset-averaged PELDOR time traces:

$$S(T) = \left(1 - \lambda \int_0^{\pi/2} P(r)(\cos(\omega_d(r,\theta)T) - 1)\sin\theta d\theta\right), \qquad (10)$$

with $P(r)$ describing the distance distribution function and λ is defined as the average of $\langle\lambda_i\rangle_v$ over all conformers i and all angles θ. The distance distribution function $P(r)$ can be obtained by solving the integral equation with a regularization procedure, e.g. Tikhonov regularization [38,36,37]. If on the other hand, the distance distribution function $P(r)$ is known, the integral kernel function can be computed numerically, allowing determination of the orientation intensity function $\lambda(\theta)$ from the original not-averaged time traces. Analysis of the angular dependence of this function on the frequency of the probe pulse might provide first qualitative information about the angle between the nitroxide plane and the inter-spin vector $\boldsymbol{r}$. Examples of this procedure will be given in the next section. If the nitroxide spin labels are rather flexible then this function will be constant with respect to θ, as explained above.

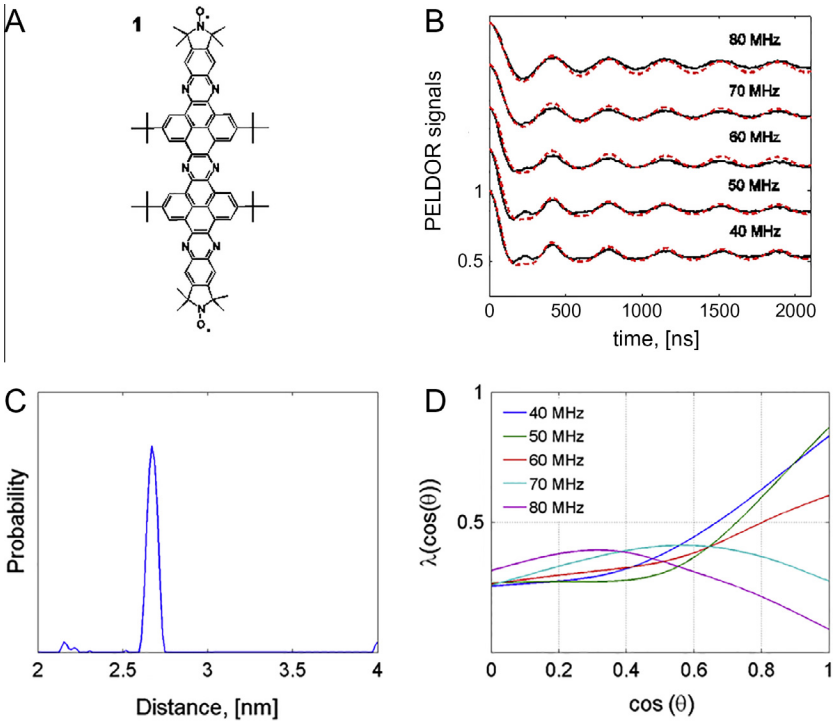

Fig. 7. Analysis of distance and orientation of rigid biradical. (A) Model biradical with a rigid orientation between both nitroxide spin labels. (B) Multi-frequency X-band PELDOR experiments (black) and best fit obtained with the PELDOR database (red). (C) Distance distribution function $P(r)$ obtained by Tikhonov regularization from the sum over all PELDOR time traces recorded with different probe frequencies ν_A. (D) Orientation function $\lambda(\theta)$ for different probe frequencies ν_A calculated numerically with the integral kernel function from the distance distribution function $P(r)$ shown in (C).

A chemical approach to separate the distance and angular information is by having two very similar spin labels, where one is rigidly attached to the nucleic acid molecule and the other can freely rotate about its N–O axis while keeping the unpaired electron spin density fixed unchanged. In the second case the distance will not be modulated but the orientation information is scrambled efficiently. Such spin labels have been called "conformationally unambiguous" [74]. We have recently synthesized such a pair of isoindoline derived spin labels, where we could show on double stranded DNA that the orientation information is almost totally gone by the one-axis rotation but can be reintroduced by stopping the rotation by an intramolecular hydrogen bond [75,76].

Simulation with the PELDOR database does not account for incomplete spin labeling or imperfections in pulse shapes, which could lead to a change in the signal modulation depth. To avoid inaccuracy in such cases, the fitting procedure can be redefined in such a way that it neglects a constant offset between experimental and fitted signal for the optimization to emphasize the change of oscillation frequency as a function of probe frequency in the simulations.

6. Application examples

The procedures explained above for predicting the geometry between two spinlabels without any pre-knowledge of the molecule was demonstrated experimentally using the rigid biradical **1** shown in Fig. 7. The model compound synthesized to evaluate our procedure [77] consists of two nitroxide spin labels rigidly aligned in such a way that the molecular axis systems of both nitroxides are coplanar and the distance vector $\boldsymbol{r}$ is aligned parallel to the molecular x-axis of both nitroxides (the N–O direction). PELDOR time traces have been recorded at X-band frequencies with offsets between pump and probe frequency ranging from 40 to 90 MHz. Comparison of the experimental multi-frequency PELDOR time traces with the synthetic spectra of the PELDOR database revealed best agreement with the simulated structure with Euler angles $\boldsymbol{o} = (0, 80°, 0)$ and a vector $\boldsymbol{r}$ of length 2.7 nm and an orientation parallel to the nitroxide x-axis, in perfect agreement with the molecular structure.

As described in the previous chapter, the orientation selection can be strongly reduced by adding up all PELDOR time traces with different probe frequency. Fig. 7 shows the distance distribution function $P(r)$ obtained by Tikhonov regularization with DEER-analyis from such an offset-averaged PELDOR time trace [38], which again nicely agrees with the known distance between the two N–O groups of the biradical. With this, the orientation intensity function $\lambda(\theta)$ can be obtained for all different probe frequencies, as shown in Fig. 7 in the lower right panel. Strong probe frequency dependent changes are observed for values of $\cos(\theta)$ close to 1 (or θ close to 0°), indicative for the given geometry of the molecule.

The geometry of this very rigid molecule can therefore be unambiguously determined by our PELDOR database approach. Similarly the distance r between the spin labels could be accurately predicted by calculation of $P(r)$ from the offset-averaged PELDOR trace. With this, the determination of the orientation functions $\lambda(\theta)$ for all different probe frequencies can be numerically obtained, which again allows the determination of the relative orientation of the distance vector $\boldsymbol{r}$ in the nitroxide molecular axis system. Thus for this very rigid molecule the distance vector $\boldsymbol{r}$ and the relative orientation $\boldsymbol{o}$ between both nitroxide moieties can be unambiguously and accurate predicted.

The situation becomes more complicated for more flexible molecules that can adapt several conformations. Compound **2** with a more flexible linker (Fig. 8) and additional rotational freedom of the two nitroxide moieties on a cone around the acetylene bond, has been used as a more complex test case. Due to this rotation, the nitroxide N–O bond direction (molecular x-axis) is distributed

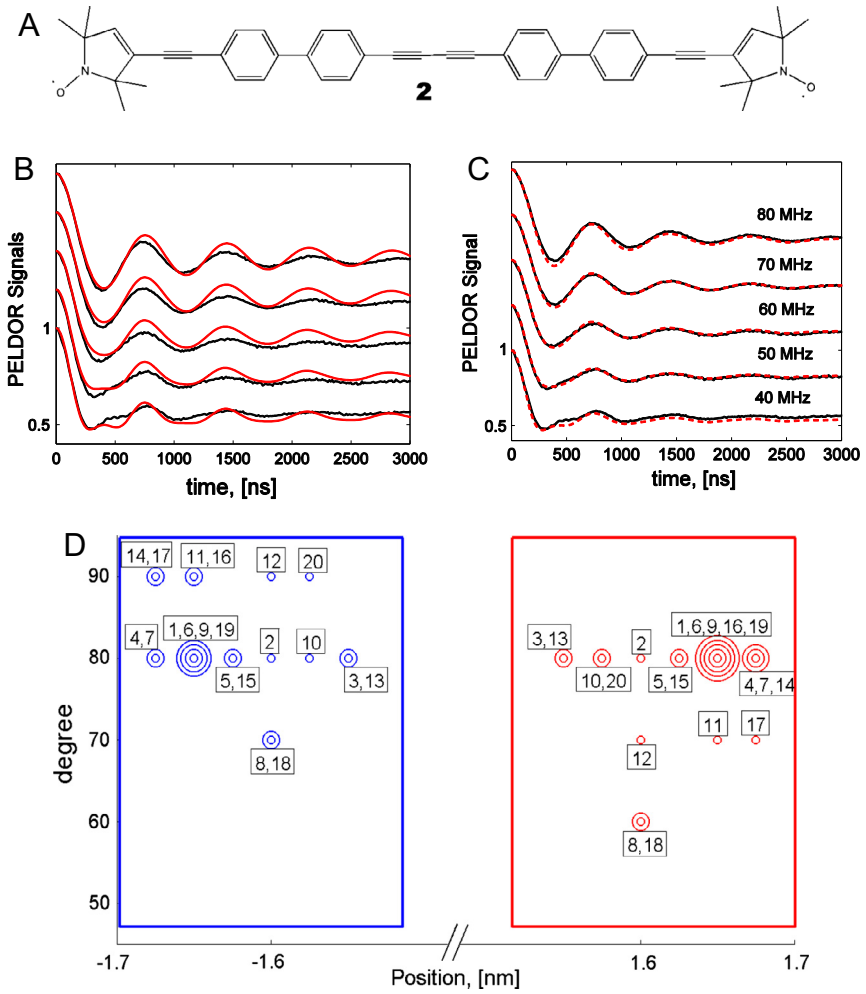

Fig. 8. Distance and conformational distribution of a flexible biradical. (A) Biradical molecule with flexible linker containing internal rotational flexibility of both nitroxide moieties. (B) Comparison of experimental PELDOR time traces at different probe frequencies (black) with simulations based on the MD trajectories (black). (C) Experimental PELDOR time traces (black) and best fit with a set of conformers from the PELDOR database (red). (D) The structure parameters of 20 conformers generating the signal consistent with the experimental data. The values of the angles β_1 and β_2 of the conformer with the number $i = 1\ldots20$ can be found as the y-coordinates of the circles marked with the number i in the left and in the right boxes respectively. The distance between the unpaired electrons in the ith conformer is obtained by subtracting x-coordinates of the ith circle in the left box from the x-coordinate of ith circle in the right box.

on a cone with opening angle of 22°, in addition to considerable bending of the linker.

Molecular dynamic studies of the molecule dissolved in a water box have been performed using the GROMACS program package with the AMBER 98 force field [78]. The equation of motion has been integrated with time steps of 2 fs over a total time span of 20 ns. Snapshots of the atomic coordinates of both nitroxides have been taken every 10 ps to create 2000 conformers. This set has been used as statistical ensemble of the molecules in the frozen sample. As can be seen (Fig. 8B) the MD simulations represent the ensemble of conformers of the biradical model compound rather well, only slightly underestimating the conformational flexibility. Applying our fitting procedure to the experimental 2D-dataset of the linear biradical resulted in an even better agreement with the experimental dataset.

The best solution is a superposition of 20 conformers, characterized by a pair of angles (β_1 and β_2), describing the angle between the nitroxide normal with respect to the distance vector $\boldsymbol{r}$, and the distance r. The other angles are in this case not determined, because only X-band PELDOR time traces have been recorded, which cannot differentiate between the molecular x- and y-axis. The parameters of the 20 conformers are tabulated with numbers in the lower panel of Fig. 8. Each conformer consists of two circles, where the y-coordinates describe the angles β_1 and β_2, respectively and the difference of the two x-values determines the distance r of this conformer. In the case of such flexible molecules it is possible that different combinations of conformer ensembles represent equally well the experimental 2D-PELDOR data set. This ambiguity can be reduced by extending the experimental data set with high-field PELDOR time traces or by further constraints from other methods, as MD, NMR or FRET.

As a first application to nucleic acid molecules we incorporated two of the rigid spinlabels Ç into double stranded DNA molecules [77]. A set of 10 molecules with the distances between the two spin labels from 5 to 14 base pairs was synthesized, PELDOR data collected and analyzed. In all cases, the mean distance and the relative orientation fit very well with predictions based on the known geometry [77,79]. Additional information about the conformational dynamics of ds-DNA was obtained by a detailed investigation of the damping of the PELDOR oscillations [56]. In this case we compared our PELDOR results with different existing models describing the dynamics of ds-DNA molecules based on modeling approaches [80], small angle X-ray scattering (SAXS) data [81], single molecule fluorescence measurements [82] or molecular dynamic simulations [83]. PELDOR experiments with six different probe frequencies (with an offset ranging from +40 to +90 MHz)

at 0.3 T and at three different spectral positions (corresponding to the g_{xx}, g_{yy} and g_{zz} position) at 6.4 T magnetic field were performed. The full set of experimental PELDOR data was then compared with simulations based on the different models: bending or twist-stretch motion with either a change in pitch height or in helix radius (Fig. 9). Only the model B with a twist-stretch motion, where the radius of the ds-DNA is modulated, agrees with our PELDOR data, whereas all the other models can be ruled out (Fig. 9). Interestingly the elasticity modulus in our experiments on short 14-mer DNA molecules is much softer compared to the fluorescence measurements, which were performed on long DNA strands, pre-stretched and attached to a magnetic bead [82]. The radius change in this 'breathing' motion of ds-DNA molecules is only of the order of 10%, meaning a change of 0.65 Å. This clearly shows the very high precision obtained with the rigid spin labels attached to the DNA molecule.

Despite the fact that we only observed the frozen-in conformational ensemble we could even prove the correlation between the twist and stretch motion of the DNA molecule by analyzing the width of the distance distribution functions $P(r)$, obtained by fitting of the offset-averaged PELDOR time traces with a Gaussian distance distribution. Whereas the average distance of the distance distribution function increases stepwise by enlarging the number of base pairs between the two spin label positions, the width of the Gaussian function has a distinct nonlinear behavior with a visible minima (Fig. 9). For the molecule with spin labels attached at position x and $x + 8$, the reduction in distance introduced by the twist motion is almost compensated by the simultaneous lengthening of the distance by the correlated stretch motion, leading to a very small distribution in distances of the conformational ensemble.

Therefore, a very detailed picture of the conformational flexibility of ds-DNA molecules has been obtained by our rigid spin label **Ç** attached to a series of DNA molecules at different positions and measured with several probe spin frequencies and at two magnetic field strengths. The data may serve as benchmark for optimization of force fields for nucleic acid molecules. Further work to investigate

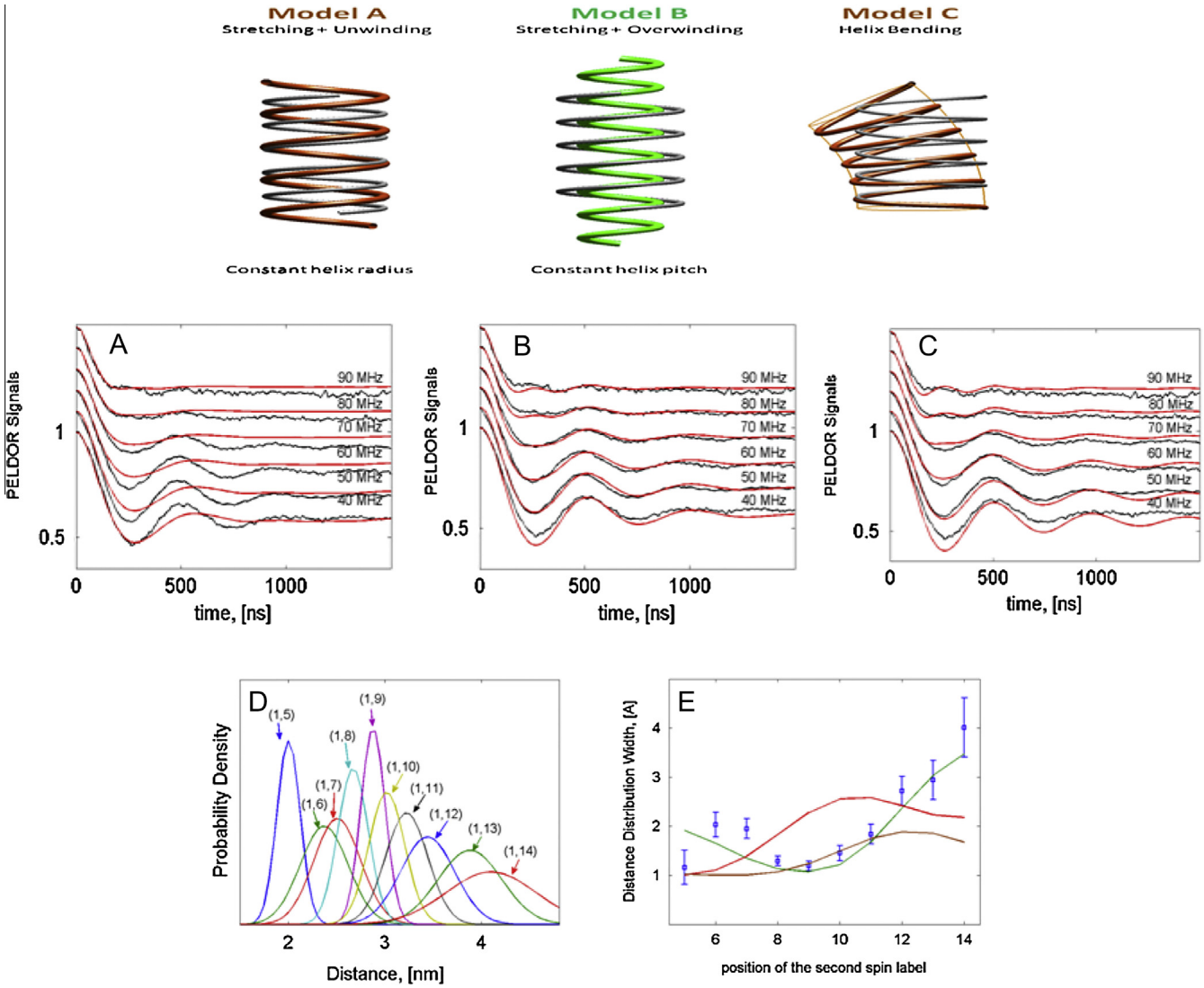

Fig. 9. Analysis of the conformational modes of double stranded DNA. Three different models are considered for the conformational dynamics of double-stranded DNA molecules: (A) change in pitch hight (red), (B) change in radius (green) and (C) bending of the helix (brown). Experimental X-band PELDOR time traces for a double-stranded DNA molecule labeled at positions 5 and 9 are shown for all three models (black) together with the best fits resulting from the different models (red). (D) Distance distribution function $P(r)$ *obtained from offset-averaged PELDOR time traces* for ten double-stranded DNA molecules labeled at positions with increasing distance between the base pairs by Gaussian fits. A minimal width of $P(r)$ was observed for the sample with eight base-pairs between the two spin labels. (E) This is only in agreement with predictions from a correlated twist-stretch motion with change in radius (model A, green line) but not with the other two models. Therefore only the model, where the radius of the double-stranded DNA molecules slightly changes with the stretching of the molecule, is consistent with all our multi-frequency/multi-field experimental PELDOR data for all 10 double labeled ds-DNA molecules.

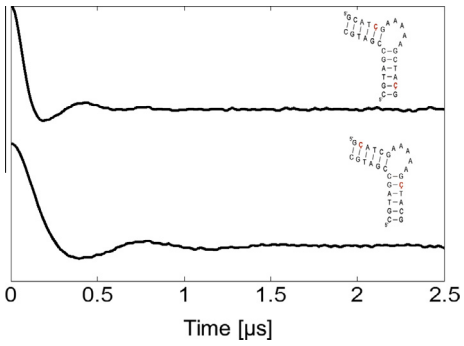

Fig. 10. PELDOR on a penta-A loop DNA molecule. PELDOR time traces taken at X-band frequencies with a pump–probe offset of 80 MHz for two different labeling positions for the **Ç** spin labels in each double-helical part of the molecule (shown in red).

the dependence of these dynamics on the specific sequence, the ionic strength or the type of ions is planned.

This procedure can now be applied to more flexible nucleic acid molecules where the rigid spin labels are incorporated into double stranded DNA helical parts of the molecule. Fig. 10 shows a demonstration on a DNA molecule with a penta-A-bulge in the center. The molecule, which has been labeled in the two double stranded parts with two rigid spin label Ç to monitor the bending and twisting of the two helical parts with respect to each other. The PELDOR time traces taken at 0.3 T magnetic field exhibit well resolved oscillations, indicating that a quantitative analysis will be also possible for such more flexible structures. It will be interesting to compare the conformational flexibility extracted from multi-frequency/multi-field PELDOR data of this molecule with structural predictions from NMR [84] and FRET experiments [9]. This work is under progress at the moment in our laboratory.

7. Conclusions and outlook

The use of rigid spin labels allows determination of not only the distance r but also the direction of this vector $\boldsymbol{r}$ and the relative orientation $\boldsymbol{o}$ between the two spin labels. This increased the number of restraints from one to six for a doubly-labeled sample. In addition, not only the number but also the quality and accuracy of the restraints get increased. Because of the rigidity of the spin label, no additional degrees of flexibility are introduced by the spin label itself. This is especially important if the conformational flexibility of the biomolecule is under investigation. This has also been recognized in protein research and new spin labels with restricted rotameric freedom have been recently developed [85].

The advantages of rigid spin labels more than compensate for the effort required for their preparation, the extended multi-frequency/multi-field PELDOR measurements and the more complicated data fitting analysis necessary to obtain full angular and distance information from rigid spin labels. This is especially useful to follow small conformational changes ore large conformational ensembles with highly flexible or partially disordered molecules. The fact that several PELDOR traces have to be taken with different probe or pump frequencies does not make these experiments more time consuming compared to PELDOR experiments with flexible spin labels, because all different offset traces can be summed up to obtain the distance distribution function $P(r)$, thus obtaining almost the same sensitivity if only this information is needed. On the other hand more detailed information is available, for example an easy check if some orientation restriction occurs which might otherwise easily lead to miss- or over-interpretation of the distance distribution function.

Another potentially important advantage of rigid nitroxide spin labels is the possibility to extend PELDOR measurements to physiological temperatures. With carbon based trityl spin labels room temperature PELDOR has already been demonstrated on immobilized lysozyme [86] and DNA [87]. With flexible nitroxide molecules this is not possible, because of the large hyperfine A-tensor anisotropy, leading to a short transversal relaxation time at room temperature due to fast rotational tumbling [86]. With the rigid spinlabel **Ç**, such motion can be suppressed if the carrying nucleic acid molecule is immobilized or large enough to tumble slowly. The possibility to incorporate spin labels into long RNA molecules by ligation techniques [88,89] as well as the investigation of RNA-protein complexes [90,88] has been already demonstrated. A rigid spin label will not only prolong the transversal relaxation time, but also allow collection of information on dynamics of biomolecules that occur on the nano- to microsecond timescale. Because the intrinsic high sensitivity of EPR, which allows experiments to be performed also in whole cells [91–94], investigations under physiological conditions (room temperature and in-cell) might be feasible in the future.

For a full and detailed description of the structure and dynamics of nucleic acid molecules a combination of different spectroscopic and computational techniques, such as NMR, EPR, fluorescence and MD simulations, will be necessary. All the spectroscopic methods have their own distance ranges and time scales so that a combination of such methods will give a more comprehensive and unique picture of the dynamics of nucleic acid molecules [90,88]. Rigid spin labels, like our **Ç** for nucleic acids, are valuable to obtain restraints with high accuracy, which is crucial for a detailed analysis of conformational dynamics of such molecules on an atomistic level.

Acknowledgments

We thank Burkhard Endeward, Olav Schiemann, Dominik Markgraf, Ivan Krstic, Sevdalina Lyubenova and Claudia Grytz for their contributions to this work. Pavol Cekan has synthesized compound **1** and the nucleic acid samples containing **Ç** and Jörg Plackmeyer has synthesized compound **2**. Financial support for this work was provided by the German Research Society (DFG), within the Collaborative Research Center CRC902 *Molecular Principles of RNA-bases Regulation* and the Iceland Research Fund.

References

[1] D. Klostermeyer, D. Hammann, RNA Structure and Folding, Biophysical Techniques and Prediction Methods, De Gruyter, 2013, ISBN 978-3-11-028495-9.
[2] H.M. Al-Hashimi, NMR studies of nucleic acid dynamics, J. Magn. Reson. 237 (2013) 191–204.
[3] A. Reining, S. Nozinovic, K. Schlepckow, F. Buhr, B. Fürtig, H. Schwalbe, Three-state mechanism couples ligand and temperature sensing in riboswitches, Nature 499 (2013) 355–359.
[4] P. Skripagdeevong et al., Structure determination on noncanonical RNA motives guided by ^{1}H NMR chemical shifts, Nat. Methods 11 (2014) 413–416.
[5] B. Furtig, C. Richter, J. Wohnert, H. Schwalbe, NMR spectroscopy of RNA, ChemBioChem 10 (2003) 936–962.
[6] J. Hennig, M. Sattler, The dynamic duo: combining NMR and small angle scattering in structural biology, Protein Sci. 23 (2014) 669–682.
[7] A. Lapinaite, B. Simon, L. Skjaerven, M. Rakwalska-Bange, F. Gabel, T. Carlomagno, The Structure of the box C/D enzyme reveals regulation of RNA methylation, Nature 502 (2013) 519–523.
[8] A. Iqbal, S. Arslan, B. Okumus, T.J. Wilson, G. Giraud, G.D. Norman, T. Ha, D.M.J. Lilley, Orientation dependence in fluorescent energy transfer between Cy3 and Cy5 terminally attached to double-stranded nucleic acids, PNAS 105 (2008) 11176–11181.
[9] A.K. Wozniak, G.F. Schroeder, H. Grubmueller, C.A.M. Seidel, F. Oesterhelt, Single-molecule FRET measures bends and kinks in DNA, PNAS 105 (2008) 18337–18342.
[10] A.D. Milov, K.M. Salikhov, J.E. Shirov, Application of the double resonance method to electron spin echo in a study of the spatial distribution of paramagnetic centers in solids, Fiz. Tverd. Tela, Leningrad 23 (1981) 975–979.

[11] A.D. Milov, A.B. Ponomarev, Y.D. Tsvetkov, Electron–electron double resonance in electron spin echo: model biradical systems and the sensitized photolysis of decalin, Chem. Phys. Lett. 110 (1984) 67–72.
[12] R.G. Larsen, D.J. Singel, Double electron–electron resonance spin–echo modulation: spectroscopic measurement of electron spin pair separations in orientationally disordered solids, J. Chem. Phys. 98 (1993) 5134–5146.
[13] R.E. Martin, M. Pannier, F. Diederich, V. Gramlich, M. Hubrich, H.W. Spiess, Determination of end-to-end distances in a series of TEMPO diradicals of up to 2.8 nm length with a new four-pulse double electron electron resonance experiment, Angew. Chem. Int. Ed. 37 (1998) 2833–2837.
[14] M. Pannier, S. Veit, A. Godt, G. Jeschke, H.W. Spiess, Dead-time free measurement of dipole–dipole interactions between electron spins, J. Magn. Reson. 142 (2000) 331–340.
[15] C. Altenbach, T. Marti, H.G. Khorona, H.G. Hubbell, Transmembrane protein structure: spin labeling of bacteriorhodopsin mutants, Science 248 (1990) 1088–1092.
[16] W.L. Hubbell, D.S. Cafiso, C. Altenbach, Identifying conformational changes with site-directed spin labeling, Nat. Struct. Biol. 7 (2000) 735–739.
[17] G. Jeschke, Determination of the nanostructure of polymer materials by electron paramagnetic resonance spectroscopy, Macromol. Rapid Commun. 23 (2002) 227–246.
[18] G. Jeschke, DEER distance measurements on proteins, Annu. Rev. Phys. Chem. 63 (2012) 419–446.
[19] O. Schiemann, T.F. Prisner, Long-range distance determinations in biomacromolecules by EPR spectroscopy, Q. Rev. Biophys. 40 (2007) 1–53.
[20] J.H. Freed, New technologies in ESR, Annu. Rev. Phys. Chem. 51 (2000) 655.
[21] P. Borbat, J. Freed, Measuring distances by pulsed dipolar ESR spectroscopy: spin-labeled histidine kinases, Methods Enzymol. 423 (2007) 52–116.
[22] S.A. Shelke, S.T. Sigurdsson, Site-directed spin labelling of nucleic acids, Eur. J. Org. Chem. 12 (2012) 2291–2301.
[23] S.A. Shelke, S.T. Sigurdsson, Site-directed spin labeling of biopolymers, Struct. Bonding 152 (2014) 121–162.
[24] A. Savitsky, A.A. Dubinskii, M. Flores, W. Lubitz, K. Möbius, Orientation-resolving pulsed electron dipolar high-field EPR spectroscopy on disordered solids: I. structure of spin-correlated radical pairs in bacterial photosynthetic reaction centers, J. Phys. Chem. B 111 (2007) 6245–6262.
[25] M.R. Seyedsayamdost, C.T. Chan, V. Mugnaini, J. Stubbe, M. Bennati, PELDOR spectroscopy with DOPA-beta 2 and NH2Y-alpha2s: distance measurements between residues involved in the radical propagation pathway of *E. coli* ribonucleotide reductase, J. Am. Chem. Soc. 129 (2007) 15748–15749.
[26] V. Denysenkov, T.F. Prisner, J. Stubbe, M. Bennati, High-field pulsed electron–electron double resonance spectroscopy to determine the orientation of the tyrosyl radicals in ribonucleotide reductase, Proc. Natl. Acad. Sci. U.S.A. 103 (2006) 13386–13390.
[27] S. Lyubenova, M.K. Siddiqui, M.J.M. Penning de Vries, B. Ludwig, T.F. Prisner, Protein-protein interaction studied by EPR relaxation measurements: cytochrome c and cytochrome c oxidase, J. Phys. Chem. B. 111 (2007) 3839–3846.
[28] V. Denysenkov, D. Biglino, W. Lubitz, T.F. Prisner, M. Bennati, Structure of the tyrosyl biradical in mouse R2 ribonucleotide reductase from high-field PELDOR, Angew. Chem., Int. Ed. 47 (2008) 1224–1227.
[29] I.M.C.V. Amsterdam, M. Ubbink, G.W. Canters, M. Huber, Measurement of a Cu–Cu distance of 26 Å by a pulsed EPR method, Angew. Chem., Int. Ed. Engl. 42 (2003) 62–64.
[30] J.S. Becker, S. Saxena, Double quantum coherence electron spin resonance on coupled Cu(II)–Cu(II) electron spins, Chem. Phys. Lett. 414 (2005) 248–252.
[31] C. Elsässer, M. Brecht, R. Bittl, Pulsed electron–electron double resonance on multinuclear metal clusters: assignment of spin projection factors based on the dipolar interaction, JACS 124 (2002) 12606–12611.
[32] M.M. Roessler, M.S. King, A.J. Robinson, F.A. Armstrong, J. Hammer, J. Hirst, Direct assignment of EPR spectra to structurally defined iron-sulfur clusters in complex i by double electron–electron resonance, Proc. Natl. Acad. Sci. U.S.A. 107 (2010) 1930–1935.
[33] A. Potapov, H. Yagi, T. Huber, S. Jergic, N.E. Dixon, G. Otting, D. Goldfarb, Nanometer-scale distance measurements in proteins using Gd^{3+} spin labels, JACS 132 (2010) 9040–9048.
[34] L. Garbuio, E. Bordignon, E.K. Brooks, W.L. Hubbell, G. Jeschke, M. Yulikov, Orthogonal spin labeling and Gd(III)–nitroxide distance measurements on bacteriophage t4-Lysozyme, J. Phys. Chem. B 117 (2013) 3145–3153.
[35] D. Banerjee, H. Yagi, T. Huber, G. Otting, D. Goldfarb, Nanometer-range distance measurement in a protein using Mn^{2+} tags, J. Phys. Chem. Lett. 3 (2012) 157–160.
[36] Y. Chiang, P. Borbat, J. Freed, The determination of pair distance distributions by pulsed ESR using Tikhonov regularization, J. Magn. Reson. 172 (2005) 279–295.
[37] Y. Chiang, P. Borbat, J. Freed, Maximum entropy: a complement to Tikhonov regularization for determination of pair distance distributions by pulsed ESR, J. Magn. Reson. 177 (2005) 184–196.
[38] G. Jeschke, G. Panek, A. Godt, A. Bender, H. Paulsen, Data analysis procedures for pulse ELDOR measurements of broad distance distributions, Appl. Mag. Res. 26 (2004) 223–244.
[39] G. Jeschke, V. Chechik, P. Ionita, A. Godt, H. Zimmermann, J. Banham, C. Timmel, D. Hilger, H. Jung, DeerAnalysis2006—a comprehensive software package for analyzing pulsed ELDOR data, Appl. Magn. Reson. 30 (2006) 473–498.
[40] G. Jeschke, M. Sajid, M. Schulte, A. Godt, Three-spin correlations in double electron–electron resonance, Phys. Chem. Chem. Phys. 11 (2009) 6580–6591.
[41] A. Giannoulis, R. Ward, E. Branigan, J.H. Naismith, B.E. Bode, PELDOR in rotationally symmetric homo-oligomers, Mol. Phys. 111 (2013) 2845–2854.
[42] B.E. Bode, D. Margraf, J. Plackmeyer, G. Durner, T.F. Prisner, O. Schiemann, Counting the monomers in nanometer-sized oligomers by pulsed electron–electron double resonance, JACS 129 (2007) 6736–6745.
[43] C. Pliotas, R. Ward, E. Branigan, A. Rasmussen, G. Hagelueken, H.X. Huang, S.S. Black, I.R. Booth, O. Schiemann, J.H. Naismith, Conformational state of the MscS mechanosensitive channel in solution revealed by pulsed electron–electron double resonance (PELDOR) spectroscopy, PNAS 109 (2012) E2675–E2682.
[44] Y. Polyhach, A. Godt, C. Bauer, G. Jeschke, Spin pair geometry revealed by high-field DEER in the presence of conformational distributions, J. Magn. Reson. 185 (2007) 118–129.
[45] B. Endeward, J. Butterwick, R. MacKinnon, T.F. Prisner, Pulsed electron–electron double-resonance determination of spin-label distances and orientations on the tetrameric potassium ion channel KcsA, J. Am. Chem. Soc. 131 (2009) 15246–15250.
[46] J.E. Lovett, A.M. Bowen, C.R. Timmel, M.W. Jones, J.R. Dilworth, D. Caprotti, S.G. Bell, L.L. Wongab, J. Harmer, Structural information from orientationally selective DEER spectroscopy, Phys. Chem. Chem. Phys. 11 (2009) 6840–6848.
[47] G.W. Reginsson, R.I. Hunter, P. Cruickshank, D.R. Bolton, S.T. Sigurdsson, G. Smith, O. Schiemann, W-band PELDOR with 1 kW microwave power: molecular geometry, flexibility and exchange coupling, J. Magn. Reson. 216 (2012) 175–182.
[48] M.D. Rabenstein, Y.K. Shin, Determination of the distance between two spin labels attached to a macromolecule, Proc. Natl. Acad. Sci. 92 (1995) 8239–8243.
[49] E.J. Hustedt, A.I. Smirnov, C.F. Laub, C.E. Cobb, A.H. Beth, Molecular distances from dipolar coupled spin-labels: the global analysis of multifrequency continuous wave electron paramagnetic resonance data, Biophys. J. 72 (1997) 1861–1877.
[50] T.R. Miller, S.C. Alley, A.W. Reese, M.S. Solomon, W.V. McCallister, C. Mailer, B.H. Robinson, P.B. Hopkins, A probe for sequence-dependent nucleic acid dynamics, J. Am. Chem. Soc. 117 (1995) 9377–9378.
[51] K.-Y. Lin, R.J. Jones, M. Matteucci, Tricyclic 2′-deoxycytidine analogs: syntheses and incorporation into oligodeoxynucleotides which have enhanced binding to complementary RNA, J. Am. Chem. Soc. 117 (1995) 3873–3874.
[52] N. Barhate, P. Cekan, A.P. Massey, S.T. Sigurdsson, A nucleoside that contains a rigid nitroxide spin label: a fluorophore in disguise, Angew. Chem., Int. Ed. Engl. 46 (2007) 2655–2658.
[53] C. Höbartner, G. Sicoli, F. Wachowius, D.B. Gophane, S.T. Sigurdsson, Synthesis and characterization of RNA containing a rigid and nonperturbing cytidine-derived spin label, J. Org. Chem. 77 (2012) 7749–7754.
[54] P. Cekan, A.L. Smith, N. Barhate, B.H. Robinson, S.T. Sigurdsson, Rigid spin-labeled nucleoside Ç: A nonperturbing EPR probe of nucleic acid conformation, Nucleic Acids Res. 36 (2008) 5946–5954.
[55] D. Sezer, S.T. Sigurdsson, Simulating electron spin resonance spectra of macromolecules labeled with two dipolar-coupled nitroxide spin labels from trajectories, PCCP 13 (2011) 12785–12797.
[56] A. Marko, V.P. Denysenkov, D. Margraf, P. Cekan, O. Schiemann, S.Th. Sigurdsson, T.F. Prisner, Conformational flexibility of DNA, J. Am. Chem. Soc. 133 (2011) 13375–13379.
[57] I. Tkach, S. Pornsuwan, C. Hobartner, F. Wachowius, S.T. Sigurdsson, T.Y. Baranova, U. Diederichsen, G. Sicoli, M. Bennati, Orientation selection in distance measurements between nitroxide spin labels at 94 GHz EPR with variable dual frequency irradiation, Phys. Chem. Chem. Phys. 15 (2013) 3433–3437.
[58] T.E. Edwards, P. Cekan, G.W. Reginsson, S.A. Shelke, A.R. Ferre-D'Amare, O. Schiemann, S.T. Sigurdsson, Crystal structure of a DNA containing the planar, phenoxazine-derived bi-functional spectroscopic probe C, Nucleic Acids Res. 39 (2011) 4419–4426.
[59] P.P. Borbat, A.J. Costa-Filho, KA. Earle, J.K. Moscicki, J.H. Freed, ESR in studies of membranes and proteins, Science 291 (2001) 266–269.
[60] I. Krstic, B. Endeward, D. Margraf, A. Marko, T.F. Prisner, Structure and dynamics of nucleic acids, Top. Curr. Chem. 321 (2012) 159–198.
[61] I. Krstic, A. Marko, C.M. Grytz, B. Endeward, T.F., Prisner, Structure and conformational dynamics of RNA determined by pulsed EPR, in: D. Klostermeier, Ch. Hammann (Eds.), RNA Structure and Folding, Biophysical Techniques and Prediction Methods, De Gruyter, 2013, pp. 261–286 (Chapter 11).
[62] Q. Cai, A.K. Kusnetzow, W.L. Hubbell, I.S. Haworth, G.P.C. Gacho, N.V. Eps, K. Hideg, E.J. Chambers, P.Z. Qin, Site-directed spin labeling measurements of nanometer distances in nucleic acids using a sequence-independent nitroxide probe, Nucleic Acids Res. 34 (2006) 4722–4730.
[63] A. Marko, V.P. Denysenkov, T.F. Prisner, Out-of-phase PELDOR, Mol. Phys. 111 (2013) 2834–2844.
[64] D. Margraf, B. Bode, A. Marko, O. Schiemann, T.F. Prisner, Conformational flexibility of nitroxide biradicals determined by X-band PELDOR experiments, Mol. Phys. 105 (2007) 2153–2160.
[65] A.D. Milov, Y.D. Tsvetkov, Double electron–electron resonance in electron spin echo: conformations of spin-labeled poly-4-vinilpyridine in glassy solutions, Appl. Magn. Reson. 12 (1997) 495–504.

[66] A.D. Milov, A.G. Maryasov, Y.D. Tsvetkov, Pulsed electron double resonance (PELDOR) and its applications in free-radicals research, Appl. Magn. Reson. 15 (1998) 107–143.
[67] A.G. Maryasov, Y.D. Tsvetkov, J. Raap, Weakly coupled radical pairs in solids: ELDOR in ESE structure studies, Appl. Magn. Reson. 14 (1998) 101–113.
[68] J. Sigg, T. Prisner, K.P. Dinse, H. Brunner, D. Schweitzer, K.H. Hausser, Electron spin echo experiments on the one-dimensional conductor $[(\text{fluoranthene})_2]^+[(PF)_x(SbF_6)_{1-x}]^-(x \sim 0.5)$, Phys. Rev. B27 (1983) 5366.
[69] M.I. Fajer, H. Li, W. Yang, P.G. Fajer, Mapping electron paramagnetic resonance spin label conformations by the simulated scaling method, J. Am. Chem. Soc. 129 (2007) 13840–13846.
[70] G.H. Rist, J.H. Hyde, Ligand ENDOR of metal complexes in powders, J. Chem. Phys. 52 (1970) 4633–4643.
[71] B.M. Hoffman, ENDOR of metalloenzymes, Acc. Chem. Res. 36 (2003) 522–529.
[72] A. Marko, T. Prisner, An algorithm to analyze PELDOR data of rigid spin label pairs, Phys. Chem. Chem. Phys. 15 (2013) 619–627.
[73] C. Abé, D. Klose, F. Dietrich, W.H. Ziegler, Y. Polyhach, G. Jeschke, H.-J. Steinhoff, Orientation selective DEER measurements on vinculin tail at X-band frequencies reveal spin label orientations, J. Magn. Reson. 216 (2012) 53–61.
[74] M. Sajid, G. Jeschke, M. Wiebcke, A. Godt, Conformationally unambiguous spin labeling for distance measurements, Chem. Eur. J. 15 (2009) 12960.
[75] D.B. Gophane, S.Th. Sigurdsson, Hydrogen-bonding controlled rigidity of an isoindoline-derived nitroxide spin label for nucleic acids, Chem. Commun. 49 (2013) 999–1001.
[76] D.B. Gophane, B. Endeward, T.F. Prisner, S.Th. Sigurdsson, Conformational restricted isoindoline-derived spin labels in dublex DNA: distances and rotational flexibility by pulsed electron-electron double resonance, Chem. Eur. J. 20 (2014) 15913–15919.
[77] O. Schiemann, P. Cekan, D. Margraf, T.F. Prisner, S. Sigurdsson, Relative orientation of rigid nitroxides by PELDOR: beyond distance measurements in nucleic acids, Angew. Chem. 48 (2009) 3292–3295.
[78] A. Marko, D. Margraf, H. Yu, Y. Mu, G. Stock, T. Prisner, Molecular orientation studies by pulsed electron–electron double resonance experiments, J. Chem. Phys. 130 (2009) 064102.
[79] A. Marko, D. Margraf, P. Cekan, S.T. Sigurdsson, O. Schiemann, T.F. Prisner, Analytical method to determine the orientation of rigid spin labels in DNA, Phys. Rev. E: Stat., Nonlinear, Soft Matter Phys. 81 (2010) 021911.
[80] N.B. Becker, R. Everaers, Comment on "remeasuring the double helix", Science 325 (2009). 538–b.
[81] R.S. Mathew-Fenn, R. Das, P.A.B. Harbury, Remeasuring the double helix, Science 322 (2008) 446–448.
[82] J. Gore, Z. Bryant, M. Nöllmann, M.U. Le, N.R. Cozzarelli, C. Bustamante, DNA overwinds when stretched, Nature 442 (2006) 836–839.
[83] B. Bouvier, H. Grubmueller, Molecular dynamic study of slow base flipping in DNA using conformational flooding, Biophys. J. 93 (2007) 770–786.
[84] U. Dornberger, A. Hillisch, F.A. Gollmick, H. Fritzsche, S. Diekmann, Solution structure of a five-adenine bulge loop within a DNA duplex, Biochemistry 38 (1999) 12860–12868.
[85] W.L. Hubbell, C.L. Lopez, C. Altenbach, Y.Z. Yang, Technological advances in site-directed spin labeling of proteins, Curr. Opin. Struct. Biol. 23 (2013) 725–733.
[86] Z. Yang, Y. Liu, Peter Borbat, J.L. Zweier, J.H. Freed, W.L. Hubbell, Pulsed ESR dipolar spectroscopy for distance measurements in immobilized spin labeled proteins in liquid solution, J. Am. Chem. Soc. 134 (2012) 9950–9952.
[87] G.Yu. Shevelev, O.A. Krumkacheva, A.A. Lomzov, A.A. Kuzhelev, O.Y. Rogozhnikova, D.V. Trukhin, T.I. Troitskaya, V.M. Tormyshev, M.V. Fedin, D.V. Pyshnyi, E.G. Bagryanskaya, Physiological-temperature distance measurements in nucleic acids using triarylmethyl-based spin labels and pulsed dipolar EPR spectroscopy, JACS 136 (2014) 9874–9877.
[88] O. Duss, M. Yulikov, G. Jeschke, F.H.T. Allain, EPR-aided approach for solution structure determination of large RNAs or protein-RNA complexes, Nat. Commun. 5 (2014), http://dx.doi.org/10.1038/ncomms4669.
[89] L. Buttner, F. Javedi-Zarhagi, C. Hoebartner, Site-specific labeling of RNA at internal ribose hydroxyl groups: terbium-assisted deoxyribozymes at work, JACS 136 (2014) 8131–8137.
[90] O. Duss, E. Michel, M. Yulikov, M. Schubert, G. Jeschke, F.H.T. Allain, Structural basis of the non-coding RNA RsmZ acting as a protein sponge, Nature 509 (2014) 588–592.
[91] R. Igarashi, T. Sakai, H. Hara, T. Tenno, T. Tanaka, H. Tochio, M. Shirakawa, Distance determination in proteins inside xenopus laevis oocytes by double electron-electron resonance experiments, J. Am. Chem. Soc. 132 (2010) 8228–9229.
[92] I. Krstic, R. Hänsel, O. Romainczyk, J.W. Engels, V. Dötsch, T.F. Prisner, Long-range distance measurements on nucleic acids in cells by pulsed EPR spectroscopy, Angew. Chem. Int. Ed. 50 (2011) 5070–5074.
[93] M. Azarkh, O. Okle, S. Singh, S.T. Seemann, J.S. Hartig, D.R. Dietrich, M. Drescher, Long-range distance determination in a DANN model system inside *Xenopus laevis* oocytes by in-cell spin-labeling EPR, ChemBioChem 12 (2011) 1992–1995.
[94] A. Martorana, G. Bellapadrona, A. Feintuch, E. di Gregorio, S. Aime, D. Goldfarb, Probing protein conformation in cells by EPR distance measurements using Gd^{3+} spin labeling, J. Am. Chem. Soc. 136 (2014) 13458–13465.